A Percolation-Theory Model of Lignin Degradation

D. F. Leclerc* and J. A. Olson

Pulp and Paper Research Institute of Canada, Vancouver Laboratory, 3800 Wesbrook Mall, Vancouver, British Columbia, V6S 2L9, Canada

Received June 11, 1991

ABSTRACT: Lignin removal during pulping is the result of the chemical degradation of two distinct cross-linked lignin gel fractions (middle lamella and secondary wall) of different polydispersities, the values of which can be predicted by gelation models. Values of the cluster-size (polydispersity) exponent, τ, were calculated using molecular-weight and gel-fraction scaling exponents obtained from the degradation data of five lignin-type models and seven pulping experiments. Results for the middle lamella agree with percolation-theory predictions (τ = 2.17) for three-dimensional condensate gels. Also, low values of the cluster-size exponent obtained during secondary-wall degradation in whole wood were in agreement with predictions given for either three-dimensional diffusion-limited cluster–cluster aggregation processes (τ = 2.00), or with percolation-theory predictions (τ = 2.05) for networks arranged in two-dimensional monolayers. However, the degradation behavior of secondary-wall lignin during pulping of wood meal and sawdust was better described by the Flory–Stockmayer model of gelation (τ = 2.50), a model which is applicable to networks having a low cross-linking density. Results for lignin-type model compounds were also interpreted with percolation and cluster–cluster aggregation models.

1. Introduction

1.1. Delignification and Lignin Degradation. Lignin may be considered to be a cross-linked amorphous polymer network, or gel, of trifunctional monomers spanning two different regions of the fiber wall, which are the middle lamella and the secondary wall. The physical structure of these regions is different, and it is generally assumed that the local lignin structure reflects this difference. The respective rates of delignification of these two regions are indeed quite variable, and those variations are a function of pulping chemistry. In addition, the macromolecular properties of soluble (sol) lignin fragments resulting from the degradation of each network are also dissimilar and may be a function of the morphology of the network.

Degradation corresponds to the breakdown of the lignin network per se in both the middle lamella and the secondary wall regions of the fiber; delignification, on the other hand, is the subsequent removal of soluble lignin fragments from both regions. Lignin degradation characteristics have been described by Szabo and Goring[1] with some success using the Flory theory of gelation,[2] in combination with the topochemical model of delignification,[1] which empirically predicts the selective removal of treelike lignin fragments from the two regions. This selective removal was first observed by Bixler.[3] The Flory theory assumes that intramolecular linkages are absent from the network. However, current knowledge about the nature of native lignin indicates that many lignin fragments do not have a treelike structure and have a significant amount of intramolecular linkages. In the present work, lignin degradation will be analyzed in terms of modern percolation concepts[4a] and compared to other suitable gelation models such as diffusion-limited cluster–cluster aggregation (CCA),[4b,c] the theory of which is well developed for rigid[4b,c] cross-linked networks. It will be shown that there is good quantitative agreement between the properties of flexible lignin fragments and those predicted by percolation theory for cross-linked networks of different polydispersities. Qualitative agreement with results predicted by cluster–cluster aggregation for rigid networks will also be discussed.

1.2. Delignification and the Pulping Process. The differences in delignification rates between the middle lamella and the secondary wall have been investigated by a number of researchers.[5-11] These studies indicate[12,13] that the time lag between the respective onset of secondary-wall and middle-lamella delignification is due to topochemical effects and is usually greatest for kraft pulping, quite small for the acid sulfite process, negligible for the early stages of chlorite delignification, and negative for Organosolv pulping.

Goring[12] also reports that the removal of lignin from the secondary wall is linked to a considerable loss of hemicellulosic materials,[14] in particular galactoglucomannan and arabinoglucuronoxylan. Such a loss is a characteristic feature of the early stages of many commercial pulping processes such as kraft and sulfite. Lignin fragments from the middle lamella contain much less hemicelluloses than secondary-wall fragments; indeed, a strong correlation exists between lignin removal from the secondary wall and the loss of hemicelluloses.[15] However, in Organosolv pulping, because of the initially slow rate of hemicellulose degradation, secondary-wall delignification does not occur until about half of the hemicellulose has been removed, along with most of the middle-lamella lignin.

Studies on diffusion effects by several workers[10,15-17] indicate that diffusion of fragments out of the network is promoted by an increase in network pore size which can be effected either by swelling agents or by the peeling reactions generated by alkali. Trapping of lignin fragments by hindered diffusion may affect the properties of the sol phase by limiting the size of fragments diffusing out of the network. These fragments are then available for further degradation after they have diffused out of the gel phase.

1.3. Lignin Degradation and Network Structure. During the initial stage of pulping, small molecular fragments are first removed from each lignin network and become soluble. Large fragments are released later. The rate of increase toward larger molecular fragments is different for each network. This trend is also less pronounced with fragments from each network obtained from a flow-through reactor than with a batch digester because sol particles released during pulping are immediately removed from the reactor and cooled, thus arresting further degradation of the sol. A similar situation arises when sol particles precipitate in batch reactors.[18] The trend toward higher sol molecular weights that is generally

0024-9297/92/2225-1667$03.00/0

observed during delignification is not seen at all during chlorite delignification, however, because of the extensive degradation of molecular fragments.

Actual structure differences between the networks are suggested by the thin, lamellar structure of the fiber wall,[13] where cellulose forms small crystalline microfibrils which are laid out in a closely-bound matrix within the secondary wall.[19] The lignin lamellae present in this microstructure are approximately 2 nm thick. This corresponds to between two and four phenylpropane monomer units. The interlamellar distance is no more than 4 times this distance.[19] Because of the geometric constraints imposed by microfibrils, lignin in the secondary wall should form a two-dimensional monolayer coating the microfibril skeleton; experimental evidence by Luner and Kempf[20] shows that lignin fragments diffusing through the cell wall mainly consist of flat, disk-shaped lamellae with a low degree of cross-linking. These lamellae would be expected to be relatively flexible and to assume an approximately spherical shape in solution. Their hydrodynamic behavior will therefore lie between that of an Einstein sphere and that of a linear non-free-draining random coil.[21] Such a picture is consistent with the native pregel lignin structure proposed by Smith et al.[22] which implies the formation of some diaryl ether cross-links by condensation during degradation. Yean and Goring[14] found, however, that condensation during sulfite pulping does not occur for secondary-wall degradation, because of the presence of sulfonate groups.

According to Flory,[23] in the absence of geometrical constraints, the stoichiometric polycondensation of difunctional linear chains with trifunctional monomers will most likely result in the formation of large tridimensional networks. Likewise, the polycondensation of two kinds of trifunctional units will most certainly generate an intricate three-dimensional network. The self-condensation of functional units along a primary chain arranged in a random coil will also produce a three-dimensional structure. Such conditions may exist in the middle lamella, where the lignin presumably forms a dense, random three-dimensional polymer gel. This polymer is rigid and insoluble in most solvents. According to Goring,[13] such a gel is noncrystalline, is optically inactive, and has a conformation in solution that is compatible with a three-dimensional structure. The thickness of lamellae in this region is more than 100 nm,[24] which increases the likelihood that such a gel will be formed.

The theory of gelation[2,23] addresses the random attachment of monomers to a macromolecule through bond formation in such a way that no cyclic structures are formed within the polymer. Degelation is considered to be the reverse of gelation[25] and reflects the random destruction of bonds within a network. Stockmayer[26] generalized Flory's theory to weakly cross-linked networks such as melt-state vulcanizates. This is now known as the Flory–Stockmayer model of gelation. Details can be found elsewhere.[23] The concept of a two-gel lignin was first proposed by Szabo and Goring.[1] The topological differences between the two gels was interpreted as a difference in rate constants. This assumption yielded a better agreement with experiment than results obtained from the single-gel model. To explain those topochemical differences, Berry and Bolker[25] and Bolker and Brenner[27] suggested that a difference in cross-linking densities of the two lignin networks accounts for the observed differences in gel reactivity and that lignin degradation can be described using the Flory theory of gelation. However, this model does not adequately explain how differences in the properties of soluble fragments such as the distribution of molecular weights and the amount of sol fractions should emerge from differences in network structure.

Investigations by Argyropoulos and Bolker[18,28-31] and by Yan[32] applied trifunctional degelation concepts to the structure of model compounds and lignin, with some success. However, Pla and Yan,[33] Yan et al.,[34] and Dolk et al.[35] determined that the critical branching coefficient, α_c, is equal to $^1/_3$ for a variety of pulping processes. According to the Flory–Stockmayer model of gelation, this corresponds to a random condensation occurring between a pair of nonterminal trifunctional *units*, which then constitutes a tetrafunctional branch *point*.[33] This contrasts with the assumption of trifunctional gelation made by Szabo and Goring, which involves linkages between nonterminal units and linear chain ends. In the following sections, we will show that a better model of lignin degradation may be provided by percolation theory,[36,37a,b] if one considers the two lignin networks to be of different polydispersities. Diffusion-limited cluster–cluster aggregation (CCA),[37c,d] a model which applies to more rigid networks[37b] and accounts for diffusion (temporal) and structural (spatial) scaling behavior of colloidal particles during gelation, will also be discussed briefly during the interpretation of results to provide a more suitable explanation for some observations. However, a more detailed description of this model lies outside the scope of this work and therefore the reader is referred to the discussion given by Vicsek.[37d]

2. Percolation Theory: Gelation/Degelation

Cross-linked networks formed from short-chain monomers or by linkages between two sites found on the same primary chain usually have a high density of cyclic structures in the form of intramolecular cross-links. The presence of these structures confers a certain rigidity to the network and causes the gelation (or degelation) process to follow a different kind of behavior from that described by the Flory–Stockmayer model.[36,37a,b] This behavior is predicted by a model based upon percolation theory, which now will be discussed in some detail.

Percolation theory[38] was first formulated as a mathematical theory for random networks and was so named because of its original application to fluid flow through random media. This theory has found many applications in fields involving random networks, including enhanced oil recovery, the formation of aerogels, and sol/gel processing of ceramics. The relationship between percolation theory and gel properties was first discussed by Stauffer[39a] and further developed by de Gennes[4a] and by Stauffer et al.:[39b] the behavior of treelike or vulcanizate networks can be extended to random, cross-linked networks. The properties of these networks can be described through scaling exponents that usually exhibit universality, which means that the values of these exponents depend only on network structure and are not affected by the details of processes at the microscopic level. Excellent reviews of percolation theory and its applications are given by Essam[40] and by Orbach.[41]

In the Flory–Stockmayer model of gelation, the polycondensation of long-chain trifunctional monomers with difunctional monomers generates a random vulcanizate network,[42] with very few cyclic linkages. The distances between available units of the same molecule are simply too great for the efficient formation of intramolecular cross-links. However, when short-chain trifunctional monomers are used instead of the long-chain units, the result is a rigid cross-linked network.

The degradation of such a network should proceed according to percolation theory for a wide range of experimental conditions.[36,43] Recently, Li[44a] discussed network degradation within the context of percolation theory. The topological character of such a network should then be reflected through scaling exponents in the value obtained experimentally for the fractal dimension of resulting fragments; these scale-invariant exponents are useful in describing the size and mass distributions of these fragments.

Mathematical analysis and computer simulation yield scaling exponents that accurately reflect the connectivity, conductivity, or rheology of a given network, which are characterized by specific values related to the dimensionality of the network.[45] Computer simulations and mathematical analysis on lattices of various shapes within a given dimensionality were all shown to yield the same universal values for these exponents.[46] Because of this insensitivity to microscopic details, we can extrapolate the behavior of a completely-ordered network such as a triangular lattice to that of a random polymer network.

There has been also much work recently regarding the application of a percolation-theory model to gelation for two- and three-dimensional polymers.[39,47] An example is the work by Adam et al.[48] that shows experimental evidence for the percolation-theory description of gelation in silica gels.

Percolation theory describes gelation as the random formation of bonds, with probability p, between nearest-neighbor monomers of functionality, f, greater than 2. Consider an initial number n^* of dissolved monomers of molecular weight M_0 per unit volume. If the number of clusters having a molecular weight M_j ($=jM_0$) is equal to n_j, the weight-average molecular weight, $\bar{M}_w^s$, of the sol phase for a given value of p is then equal to $(\sum_j n_j M_j^2/\sum_j n_j M_j)$. For $p < P_c$, a polydisperse population of finite sol clusters forms and grows until a treelike spanning cluster (gel) appears at a critical point, P_c. The value of the gel point for network structures depends on the value of f and on whether polycondensation or self-condensation is occurring. The gel point is also called the percolation threshold. Beyond the gel point ($p \geq P_c$), the proportion of intramolecular links steadily increases[49] until a maximum cross-linking density, δ, is reached, and there is an ever-decreasing fraction, W^s, of ever-smaller sol clusters which progressively attach themselves to the gel as p tends to unity. The low cross-linking density found at the gelation point can be preserved if, shortly after gelation, carboxyl ends are reacted with diphenyldiazomethane (DDM)[49] to form stable benzhydryl groups. Otherwise, postgel reactions will generate loops throughout the gel, thus creating a percolation network. Degelation proceeds in reverse from $p = 1$ to $p = P_c$. From graph theory, we first adopt Flory's definition of the critical branching coefficient, α_c, as the gel point for a spanning cluster created by monomers of average functionality f:

$$\alpha_c = 1/(f-1) \tag{1}$$

The dimensionless extent of degradation can then be defined as

$$\epsilon = \left|\frac{p - P_c}{P_c}\right| \tag{2}$$

where $P_c \leq p \leq 1$ for degelation. In lignin networks or primary chains, self-condensation prevails and therefore $\alpha = p$, with f being equal[33] to 4. The following relationship between p and W^s then applies:[50]

$$p = [0.75 + \{0.5 + (W^s)^{1/4}\}^2]^{-1} \tag{3a}$$

with $P_c = 0.333$. This value of the gelation point has been obtained experimentally for lignin with good precision by plotting the extent of reaction, p, against the reciprocal of $\bar{M}_w^s$ and extrapolating[33,35] to $[\bar{M}_w^s]^{-1} = 0$. For trifunctional polycondensates, $\alpha = p^2$ and eq 3a becomes[1,23]

$$p = [1 + (W^s)^{1/3}]^{-1/2} \tag{3b}$$

with $p = \alpha^{1/2}$ and $P_c = 0.707$. For the random cross-linking of primary chains of a given cross-linking density δ, the relationship between p and W^s is[51]

$$p = [1 + \delta\{(0.5 + (W^s)^{1/2})^2 - 0.25\}]^{-1} \tag{3c}$$

with $P_c = [1 + 2\delta]^{-1}$, as reported by Flory.[23] Beyond the gelation point, the fraction of monomers, W^g, found in the gel increases monotonically until all monomers are incorporated in the gel:

$$W^g = \epsilon^{\beta_d} \qquad (d \in \{2,3\}) \tag{4a}$$

where d represents the geometrical dimensionality of the network and β_d is the order-parameter exponent[52] that measures the extent of gel formation beyond the gelation point. For percolation theory, the value of β is significantly lower than unity. This contrasts with the prediction of a value of unity for β made by Flory.[23] Percolation theory thus permits a smaller sol fraction beyond the gelation point than that predicted by the Flory–Stockmayer model. The sol–gel transition is much more sudden for percolation theory, with gel breakdown occurring much more quickly near gelation. The probability that a monomer is contained in the sol is then

$$W^s = 1 - \epsilon^{\beta_d} \tag{4b}$$

Consider a basic cross-linking unit containing Z monomers having an arbitrary length, which is set here to unity. The radius of gyration, ξ, of the finite sol clusters[52] then increases as the gelation point is approached from above or below and is given by

$$\xi = Z^{1/2}\epsilon^{-\nu_d} \tag{5}$$

where ν is the correlation-length scaling exponent. The value of Z determines the range of percolation behavior.[37a] Percolation behavior generally occurs if the value of Z is on the order of a few units. When Z is large enough for cross-links to occur infrequently along polymer chains, percolation behavior breaks down and gelation proceeds according to the Flory–Stockmayer theory. For a given dimensionality, the weight-average molecular weight, $\bar{M}_w^s$, of the sol clusters also increases near the gelation point:[48]

$$\bar{M}_w^s \simeq ZM_0\epsilon^{-\gamma_d} \tag{6}$$

where γ is the molecular-weight exponent, which is greater than unity for percolation networks. $M_0 \sim 200$ g/mol for a phenylpropane unit. For degelation, the possibility of condensation reactions occurring as diaryl ether cross-links[22] between sol clusters must be addressed. We assume that the probability of such reactions is proportional to ϵ, which is a linear function of the probability of bond formation, p. Therefore, eq 6 can be modified as follows:

$$\bar{M}_w^s - ZM_0\epsilon^{1-\gamma} \tag{7}$$

where the subscript is hereafter omitted for clarity. Equation 7 also applies to a degradation process which is carried out in a flow-through reactor or which is accompanied by precipitation of the sol fraction. The fragments

Table I
Theoretical Values of Scaling Exponents for the Flory–Stockmayer and Percolation-Theory Models[a]

exponent	Flory–Stockmayer ($d = 6$)	percolation ($d = 2$)	percolation ($d = 3$)
β^*	1.00	0.14	0.39
γ^*	1.00	2.39	1.89
ν^*	0.50	1.33	0.89
D_p^*	4.00	1.90	2.56
τ^*	2.50	2.05	2.17
D_a	2.00	1.60	2.00

[a] References 37a, 52, 55, and 56.

are thus protected from any subsequent degradation or condensation,[18] and the resulting higher sol molecular weight reflects the fact that no further cleavage of sol–sol bonds is taking place. The number of unbroken bonds is thus lower and therefore results in an increase in the value of $\bar{M}_w^s$ that is also proportional to ϵ.

The *fractal dimension*, D_p, of the polydisperse branched polymers in the reaction bath can be calculated experimentally using scaling laws that describe relationships between the exponents β, γ, and ν.[45,52] Hence

$$D_p = (\gamma + \beta)/\nu \tag{8}$$

Theoretical values for the scaling exponents of eq 8 are summarized in Table I. Theoretical values of percolation exponents are identified throughout the text with a starred superscript. A more detailed discussion of these values is provided by Daoud et al.,[37a] Wilkinson and Willemsen,[46] and Gould and Tobochnik.[52] Percolation theory also predicts that, for a given distance, ϵ, to the gelation threshold, the probability, $\rho_j(\epsilon)$, of finding in a particular fraction large sol fragments having a given molecular weight, M_j, is equal to[48]

$$\rho_j(\epsilon) = n_j(\epsilon)/n^* = [M_j]^{-\tau} f(\epsilon[M_j]^{\sigma}) \tag{9}$$

where M_j is large, σ is a cutoff exponent ($=[\phi\nu]^{-1}$), and $f(x)$ is an exponentially-decaying function which rapidly cuts off the polydisperse cluster-size distribution, $\rho_j(\epsilon)$, above a characteristic molecular weight, M^* ($=ZM_0\epsilon^{(1/\sigma)}$). Hence x is equal to $(M_j/M^*)^{\sigma}$. Using previous definitions for ζ, W^g, and $\bar{M}_w^s$, M^* may also be written as $(\bar{M}_w^s)^{1+(\beta/\gamma)}$, $(\bar{M}_w^s)^{1/(3-\tau)}$, or, more simply, $[\bar{M}_w^s/W^g]$. In percolation theory, the cluster-size exponent τ is a dimension-dependent parameter which is equal to 2.054 for two dimensions and 2.170 for three dimensions.[52] For percolation clusters, the value of τ is related to the geometrical dimensionality, d, of the network and to the fractal dimension, D_p, of the sol clusters by the following hyperscaling relationship:[46]

$$\tau = \frac{d + D_p}{D_p} \tag{10}$$

The principal characteristic of a fractal cluster is the presence within its boundaries of voids having a wide range of sizes, which causes the cluster to have a much smaller density than a compact, solid network. The density within a fractal cluster decreases steadily with the cluster molecular weight, $\bar{M}_w^s$. This is not the case for the density of random or nonscaling structures which remains constant, because their mass follows an integer-squared or cubed-exponential relationship. For three-dimensional structures, the voids within a fractal cluster will make such a structure partially susceptible to swelling when immersed in semidilute solutions. The clusters in the reaction bath tend to overlap and interact with each other. As long as this interaction remains substantial, hyperscaling still holds and the fractal dimension of the ensemble of polydisperse clusters is given experimentally by the following ratio of percolation exponents:

$$\phi = \frac{\gamma}{\nu(3 - \tau)} \qquad (\phi \le D_p) \tag{11a}$$

where the value of τ does not depend on swelling conditions. If little or no swelling occurs during the course of lignin degradation, hyperscaling prevails and ϕ is then equal to its percolation value, D_p, as indicated in Table I. For intermediate swelling, we can calculate ϕ using eq 8 and $\phi = D_p$ since swelling will affect the values of both γ and β and then estimate τ by inserting the experimental value of ϕ in eq 11a.

Whereas linear polymers adopt a low-energy, random-walk configuration in dilute solutions, the situation is slightly different for branched polymers, which tend to swell very strongly upon dilution. Because of this strong swelling, hyperscaling no longer applies: the fractal dimension of the branched polymers drops to a value close to that of *lattice animals*.[37b] This occurs in the strong swelling limit because of the much larger volume occupied by the solvent. This fractal dimension is independent of the values given for percolation exponents. The value of the fraction dimension, D_a, of a monodisperse ensemble of *fully-swollen* clusters is then equal to its Flory estimate:

$$D_a = \frac{2(d + 2)}{5} = 2 \qquad (d = 3) \tag{11b}$$

For tridimensional classical gelation D_a is therefore approximately equal[37a,b] to $D_p^*/2$. For polydisperse ensembles the effective dimension becomes equal to $D_a(3 - \tau)$, a value observed in scattering experiments.[37b] If a significant number of cross-links are broken and if the cluster is immersed in a good solvent, the value of ϕ will approach the value of D_p for a two-dimensional percolation network. The swelling process is then similar to laying flat a crumpled sheet of paper, and the value of τ for two dimensions is easily calculated by substituting ϕ for D_p in eq 10. Conversely, a poor solvent may force a two-dimensional percolation cluster to assume a three-dimensional configuration. Rearranging eq 10 yields the fractal dimension, D_p, of the percolation clusters that constitute the macromolecular network:

$$D_p = d/(\tau - 1) \tag{12}$$

If the ensemble is monodisperse ($\tau = 2$), there is no scaling of void sizes and clusters tend to fill all of the available space. Therefore, $D_p \simeq d$.

Viscometric measurements represent yet another way of estimating the fractal dimension of partially-swollen clusters[44a,53] for a given solvent, through the Mark–Houwink exponent, α', the value of which is dependent on the viscometric fractal dimension, D_v, of partially-swollen clusters. The Mark–Houwink exponent is related to the intrinsic viscosity, $[\eta]$, of the solution by

$$[\eta] = (\bar{M}_w^s)^{\alpha'} \tag{13}$$

The Mark–Houwink exponent is zero for an Einstein sphere, approximately 0.15 for a rigid, cross-linked network, between 0.5 and 0.8 for a non-free-draining coil, 1.0 for a free-draining coil, and 1.8 for rigid, linear rods.[12] This exponent is related to the viscometric fractal dimension, D_v, of partially-swollen clusters by the following:[44a,53]

$$D_v = 3/(1 + \alpha') \tag{14}$$

This suggests that the fractal dimension for linear rods is not equal to unity, but should have a value of 1.07

Table II
Values of Critical Parameters Pertaining to the Degradation/Pulping Behavior of Selected Cross-Linked Networks

expt	network	f	α_c	P_c
1[a]	BTA/DMG	3.000	0.500	0.707
2[b]	BTA/HDG (in THF)	3.000	0.500	0.707
3[b]	BTA/HDG (in MeOH)	3.000	0.500	0.707
4[c]	P_s-COOH/DMG (δ = 0.152)		0.767	0.767
5[c]	P_s-COOH/DMG (δ = 0.40)		0.555	0.555
6[d]	dioxane/HCl spruce I	4.000	0.333	0.333
7[e]	dioxane/HCl spruce II	4.000	0.333	0.333
8[f]	sulfite spruce	4.000	0.333	0.333
9[g]	sulfite II spruce/fir	4.000	0.333	0.333
10[h]	kraft I	4.000	0.333	0.333
11[i]	kraft II	4.000	0.333	0.333
12[j]	chlorite	4.000	0.333	0.333

[a] Reference 57. [b] Reference 18. [c] Reference 30. [d] Reference 32 (batch/sawdust). [e] Reference 33 (flow-through/wood meal). [f] Reference 14 (flow-through/sawdust). [g] Reference 58 (flow-through/spent liquor). [h] Reference 59 (flow-through/sawdust). [i] Reference 35 (flow-through/whole wood). [j] Reference 15 (flow-through/wood meal).

according to the value for α' given by Goring.[12] The intrinsic viscosity of a diluted sol was also evaluated by Daoud et al.[44b] Further verification of percolation behavior can then be carried out by comparing the results for ϕ (eq 11a) to confirm the correct choice for the correlation-length exponent, ν.

3. Analysis of Experimental Data

Molecular-weight, gel-fraction, and viscometric data published by several researchers for the polymerization or degradation of lignin and lignin-type models (see Table II) were analyzed and interpreted below within the context of percolation theory. The Flory–Stockmayer model was treated as a special case of percolation. Twelve different systems are shown in Table II in numerical order, along with the reference for each system. The lignin-type models are benzenetriacetic acid–decamethylene glycol copolymer (BTA/DMG), benzenetriacetic acid–hexadecamethylene glycol copolymer (BTA/HDG), and acid-functionalized polystyrene (P_s-COOH) cross-linked with DMG using two different cross-linking densities. DDM was not used during the synthesis of these networks. In addition, two data sets were analyzed for each of the following pulping processes: Organosolv, sulfite, and kraft. One set of gel-fraction and molecular-weight results was also available for chlorite delignification. The first six experiments were conducted in batch reactors. Precipitation of the sol phase in experiment 3, however, created a situation similar to that found in a flow-through reactor.[18] Pulping experiments 7, 8, 10, 11, and 12 were conducted in flow-through reactors, with the lignin fractions analyzed for average molecular weight. Experiment 9 was also conducted in a flow-through reactor, but with the total collected lignin analyzed for molecular weight by a dialysis method. Functionalities and gel points (Table II) were taken from either original or subsequent references or were calculated with the method given in Pla and Yan.[33] Gel points for the two cross-linked networks were calculated using eq 3c and setting W_c^s equal to unity. Gel-fraction values for degradation and pulping experiments were obtained from sol-fraction and delignification percentages, respectively. The extent of reaction, p, was obtained using eq 3a for f = 4, eq 3b for f = 3, or eq 3c for the two values of δ. The topochemical model predicts that sol fragments from either the secondary wall or the middle lamella predominate in the early phase of degradation, while a greater amount of sol fragments from the other region is found toward the end of the degradation. The order in which these fragments appear depends on the pulping method. For example, in sulfite pulping, fragments from the secondary wall appear first, while in Organosolv these fragments are detected late in the process. Consequently, early- and late-phase data were fitted separately where applicable, with the best linear fit for β and γ determined at each end of the data set. Experimental estimates of γ were obtained by log–log least-squares analysis using eq 6 for batch systems and eq 7 for flow-through systems or condensation reactions (Table III). Equation 4a was used to calculate the gel-fraction exponent β, also by least-squares analysis. Then, given that only three different theoretical values of D_p are possible, the three choices of ν given in Table I were tested in eq 8 with the experimental values of β and γ given in Table III, with the closest match for D_p* accepted. Results for experimental and theoretical values of D_p and τ (obtained from eq 10) are shown in Tables IV and V, respectively. These parameters can distinguish between the two types of lignin and permit the verification of previous assignments made by topochemical studies. Results for ϕ obtained from eq 11a are also tabulated in Table VI and compared with the viscometric value, D_v, obtained from eq 14.

4. Results and Discussion

4.1. Scaling Exponents. Values of β, γ, and ν are given in Table III. The logarithm of the gel fraction, W^g, during degelation of theoretical percolation networks is plotted against the logarithm of ϵ in Figure 1 as solid curves for each of the three values of β given in Table I. These curves have slopes which are equal to β, where the values of β correspond to two-dimensional [2D], three-dimensional [3D], and Flory–Stockmayer [FS] degelation, respectively. Data points are also shown in Figure 1 for the three typical experimental degradation experiments. These are BTA/HDG polycondensate degradation, dioxane/HCl pulping of spruce meal, and kraft pulping of hemlock chips. The curves representing degradation of two- and three-dimensional percolation networks are closer to experiments than that representing Flory–Stockmayer degelation.

A change in the value of β is seen in the evolution of log W^g versus log ϵ (dashed lines) for kraft pulping of hemlock chips, indicating that two different types of polymer networks are degraded during pulping. This is found for all sulfite and kraft pulping experiments (Table III). No change in slope was observed for dioxane/HCl, perhaps because pulping was not done beyond 60% delignification and not enough data were available to identify a second slope. Only one type of network was present in the BTA/HDG system (experiment 2); hence, no change of slope occurred. The logarithm of the lignin molecular weight, $\bar{M}_w^s$, is plotted in Figure 2 against the logarithm of ϵ. A similar change in the slope, γ, to that observed in Figure 1 for β is observed for kraft pulping of hemlock chips. All sulfite and kraft pulping experiments follow suit. This is compatible with a bimodal distribution[13] of molecular weights, which would correspond to fragments from two-dimensional monolayers in the secondary wall and from a three-dimensional middle lamella, respectively.

Although two distinct polymer networks were observed in sulfite and kraft pulping, the values of β and γ (Table III) do not match the theoretical values given in Table I for two- and three-dimensional lignin or those given for the Flory–Stockmayer model. These discrepancies are

Table III
Values of Scaling Exponents Obtained from Degradation/Pulping Experiments Performed on Selected Cross-Linked Networks

expt	network		β[a]	γ[c]	ν[d]	remarks
1	BTA/DMG (δ = 1.00)		0.65	1.90[c]	1.33	polymerization
2	BTA/HDG (in THF) (δ = 1.00)		0.27	2.25[c]	1.33	degradation in a good swelling solvent
3	BTA/HDG (in MeOH)	a[h]	0.35	2.19[c]	1.33	degradation/precipitate in a poor nonswelling solvent
		b	0.59	1.74[b]	0.89	
4	P_s-COOH/DMG (δ = 0.15)		0.88	1.07[c]	0.50	low cross-linking density (Flory–Stockmayer)
5	P_s-COOH/DMG (δ = 0.40)		0.84	1.51[b]	0.89	high cross-linking density (3D percolation)
6	dioxane/HCl spruce I		0.61	1.68[c]	0.89	middle lamella[e] (batch/sawdust)
7	dioxane/HCl spruce II		0.62	1.71[b]	0.89	middle lamella[e] (flow-through/wood meal)
8	sulfite I	a	0.65	1.29[c]	0.50	secondary wall[e]
	spruce	b	0.90	1.36[b]	0.89	middle lamella[e] (flow-through/sawdust)
9	sulfite II	c	0.73	1.32[c]	0.50	secondary wall[e]
	spruce/fir	c	0.39	1.86[b]	0.89	middle lamella[e] (dialysis/spent liquor)
10	kraft I	a	0.64	1.34[b]	0.50	secondary wall[e]
	spruce	b	0.85	1.57[b]	0.89	middle lamella[e] (flow-through/sawdust)
11	kraft II	a	0.55[f], 0.54	1.97,[g] 2.01[b]	1.33	secondary wall[e]
	hemlock	b	0.88	1.47	0.89	middle lamella[e] (flow-through/whole wood)
12	chlorite	a	0.43	1.00[b]	1.33	secondary wall[e]
		b	0.70	1.00[b]	0.89	middle lamella[e] (flow-through/wood meal)

[a] Equation 4a. [b] Equation 7 (flow-through, etc). [c] Equation 6 (batch). [d] Table I. [e] Topochemical data. [f] $(M^*/\bar{M}_w{}^s) = \epsilon^{-\beta}$. [g] $(W^sM^*) = \epsilon^{1-\gamma}$. [h] (a) Early phase; (b) late phase; (c) dialysis.

Table IV
Values of Fractal Dimensions Pertaining to the Degradation/Pulping Behavior of Selected Cross-Linked Networks

expt	network		D_p[a]	D_p*	best model
1	BTA/DMG		1.91	1.90	percolation (d = 2) or DLCCA
2	BTA/HDG (in THF)		1.89	1.90	percolation (d = 2) or DLCCA
3	BTA/HDG (in MeOH)	a[d]	1.91	1.90	percolation (d = 2) or DLCCA
		b	2.63	2.56	percolation (d = 3)
4	P_s-COOH/DMG (δ = 0.15)		3.90	4.00	Flory–Stockmayer
5	P_s-COOH/DMG (δ = 0.40)		2.59	2.56	percolation (d = 3)
6	dioxane/HCl spruce I		2.58	2.56	percolation (d = 3)
7	dioxane/HCl spruce II		2.62	2.56	percolation (d = 3)
8	sulfite I	a	3.88	4.00	Flory–Stockmayer
	spruce	b	2.54	2.56	percolation (d = 3)
9	sulfite II	c	4.09	4.00	Flory–Stockmayer
	spruce/fir	c	2.56[b]	2.56	percolation (d = 3)
10	kraft I	a	3.96	4.00	Flory–Stockmayer
	spruce	b	2.71	2.56	percolation (d = 3)
11	kraft II	a	1.90[c]	1.90	percolation (d = 2) or DLCCA
	hemlock	b	2.63	2.56	percolation (d = 3)
12	chlorite	a	1.07	1.00	linear rods (d = 1)
		b	1.90	1.90	DLCCA

[a] Equation 8. [b] Equation 12. [c] Best of two values in Table III. [d] (a) Early phase; (b) late phase; (c) dialysis.

probably due to the fact that hindered diffusion through the primary and secondary walls limits the size of sol particles available for further degradation. This should result in a lower value of γ and an increased value of β, as observed. Also, the continued degradation of sol particles involves fewer cross-links and probably follows the Flory–Stockmayer model more closely—hence the higher value for the gel-fraction exponent, β. This should be especially true for fragments that appear late in the pulping process.

4.2. Fractal Dimensions and Cluster-Size Exponents. Calculated values of the fractal dimension, D_p, are given in Table IV, along with the theoretical value, D_p*, derived from the model that offers the best description of the results. The fractal dimension, D_p, of the sol clusters reflects the hyperscaling character of the degradation process; when $\phi = D_p$, its value can also be calculated through eq 11a, which describes the theoretical relationship between experimental values of the scaling exponents γ and ν. The results shown in Table IV suggest a fractal dimension which is predicted by either two- ($[D_p^*]_{d=2}$ = 1.90) or three-dimensional ($[D_p^*]_{d=3}$ = 2.56) percolation, and by Flory–Stockmayer gelation. The result for Flory–Stockmayer gelation ($[D_p^*]_{d=6}$ = 4.00) was first obtained by Zimm and Stockmayer[54] and reflects the competition between a very close packing and the small contribution by individual chains to the overall density.[37a]

Values calculated for the cluster-size exponent, τ, are given in Table V. Results for the middle lamella agree with percolation-theory predictions (τ^* = 2.17) for three-dimensional condensate gels. Also, values of the cluster-size exponent obtained during secondary-wall degradation in whole wood also were in agreement with either percolation-theory predictions (τ^* = 2.05) for networks arranged in two-dimensional monolayers or predictions given for a diffusion-limited cluster–cluster aggregation (DLCCA) process (τ^* = 2.00). However, the degradation behavior of secondary-wall lignin during pulping of wood meal and sawdust was better described by the Flory–Stockmayer model of gelation (τ^* = 2.50), a model which is applicable to networks having a low cross-linking density. Results for lignin-type models also followed percolation-theory predictions, except for experiment 4, which followed the Flory–Stockmayer model because of its low cross-linking density. The difference between experimental and theoretical values is no more than 2.5%, with most results being 1% or less. The value of τ does not seem to change with the pulping process; nevertheless, it does depend on cluster polydispersity.

Table V
Comparison of Experimental and Theoretical Values for the Cluster-Size Exponent τ

expt	network		τ[a]	τ^*	% diff	remarks
1	BTA/DMG		2.049	2.054	0.24	percolation (d = 2) or DLCCA
2	BTA/HDG (in THF)		2.058	2.054	0.24	percolation (d = 2) or DLCCA
3	BTA/HDG (in MeOH)	a[d]	2.050	2.054	0.20	percolation (d = 2) or DLCCA
		b	2.142	2.170	1.29	percolation (d = 3)
4	P_s-COOH/DMG (δ = 0.15)		2.538	2.500	1.54	Flory–Stockmayer
5	P_s-COOH/DMG (δ = 0.40)		2.157	2.170	0.60	percolation (d = 3)
6	dioxane/HCl					
	spruce I		2.164	2.170	0.28	percolation (d = 3)
7	dioxane/HCl					
	spruce II		2.147	2.170	1.06	percolation (d = 3)
8	sulfite I	a	2.545	2.500	1.80	Flory–Stockmayer
	spruce	b	2.180	2.170	0.46	percolation (d = 3)
9	sulfite II	c	2.498	2.500	0.08	Flory–Stockmayer
	spruce/fir	c	2.173[b]	2.170	0.14	percolation (d = 3)
10	kraft I	a	2.520	2.500	0.80	Flory–Stockmayer
	spruce	b	2.105	2.170	2.30	percolation (d = 3)
11	kraft II	a	2.058[c]	2.054	0.20	percolation (d = 2) or DLCCA
	hemlock	b	2.139	2.170	1.34	percolation (d = 3)
12	chlorite	a	N/A	N/A		linear rods (d = 1)
		b	2.053	2.054	0.05	DLCCA

[a] Equation 10. [b] Equation 11a. [c] Best of two values in Table III. [d] (a) Early phase; (b) late phase; (c) dialysis.

Table VI
Values of Fractal Dimensions Pertaining to the Viscosity Behavior of Solvated Cross-Linked Networks

expt	network		D_v[a]	ϕ[b]	remarks
1	BTA/DMG		2.61[d]	2.24[j]	
2	BTA/HDG (in THF)			2.68[j]	
3	BTA/HDG (in MeOH)	a[k]		2.59[j]	
		b		2.29	
4	P_s-COOH/DMG (δ = 0.40)			1.95[i]	
5	P_s-COOH/DMG (δ = 0.40)			2.12	
6	dioxane/HCl				
	spruce I		2.61[e]	2.26	
7	dioxane/HCl				
	spruce II		2.61[e]	2.25	
8	sulfite I	a	2.04[f]	1.94[i]	secondary wall
	spruce	b		1.87	middle lamella
9	sulfite II	c	2.04[f]	2.04[i]	secondary wall
	spruce/fir	c		2.52[c]	middle lamella
10	kraft I	a	2.27[g]	1.98[i]	secondary wall
	spruce	b		1.97	middle lamella
11	kraft II	a	2.27[g]	2.37[j]	secondary wall
	hemlock	b		1.91	middle lamella
12	chlorite	a	1.07[h]	1.16[j]	secondary wall
		b		1.90[c]	middle lamella

[a] Equation 14. [b] Equation 11a. [c] Equation 8, $\phi = D_p$. [d] References 28 and 49. [e] Reference 60. [f] References 58 and 62. [g] References 61 and 63. [h] Equation 14, $\alpha' = 1.8$. [i] $\phi = D_p/2$. [j] $\nu^* = 0.89$. [k] Early phase; (b) late phase; (c) dialysis.

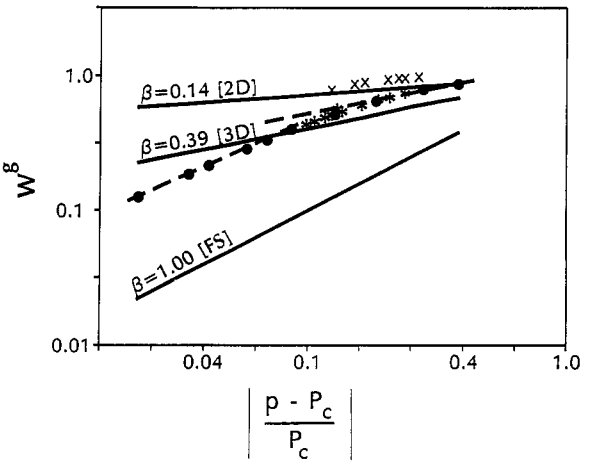

Figure 1. Evolution of the logarithm of the gel fraction, W^g, versus the logarithm of the extent of reaction, ϵ: (×) BTA/HDG in THF;[18] (●) kraft pulping of hemlock wood chips;[35] (*) Organosolv pulping of spruce meal.[33] Theoretical curves are shown for the two-dimensional secondary-wall [2D] (β = 0.14) and three-dimensional middle-lamella [3D] (β = 0.39) percolation network and for Flory–Stockmayer gelation [FS] (β = 1.00). Experimental slopes for kraft pulping of hemlock chips are shown by dashes.

The good agreement of pulping experiments with the theoretical values given in Table I also supports the concept of tetrafunctional branch points in sol lignin.[33] This has been established by Pla and Yan[33] and confirmed by Dolk et al.:[35] the branching probability was plotted against the reciprocal of $\bar{M}_w^s$. The graph was then extrapolated to $(\bar{M}_w^s)^{-1} = 0$ to obtain the gelation point at $p_c = 0.33 \pm 0.01$. These branch points may be formed by condensation reactions within the gel during pulping, and it is possible that these branch points do not occur in native lignin.

The diffusion-limited cluster–cluster aggregation model (DLCCA)[37c,d] may also provide a better physical explanation than any other interpretation available for two-dimensional percolation because it makes predictions for tridimensional aggregates. The size distribution of these aggregates is known to be much less polydisperse than for percolation clusters.[37c,d] Also, because this process is diffusion-limited, a natural explanation would be available for the observed differences in delignification rates during kraft and Organosolv pulping between the secondary wall and the middle lamella. A detailed description must be deferred until further work is carried out. Even though the scaling behavior of trifunctional lignin-type models is compatible with two-dimensional percolation, these results may also agree with DLCCA predictions; for example, the degradation of BTA/DMG and BTA/HDG networks results in cluster distributions of low polydispersity. Experiments 4 and 5 confirmed Flory's prediction that high cross-linking densities in randomly-coiled condensates of acid-functionalized linear polymers result in three-dimensional networks, while low cross-linking densities produce loose structures similar to those found in melt-state vulcanizates, for which degradation conforms to Flory–Stockmayer gelation. The observed trend of molecular weights in experiment 5 followed eq 7, which indicates that association by intermolecular condensation may be occurring because of the presence of free, non-methylated acid groups at chain ends.[30]

4.3. Analysis of Viscometric Data. In general, most of the values of D_v listed in Table VI indicate hydrodynamic behavior which lies between that of an Einstein sphere (D_v = 3) and that of a non-free-draining coil (D_v = 2), as

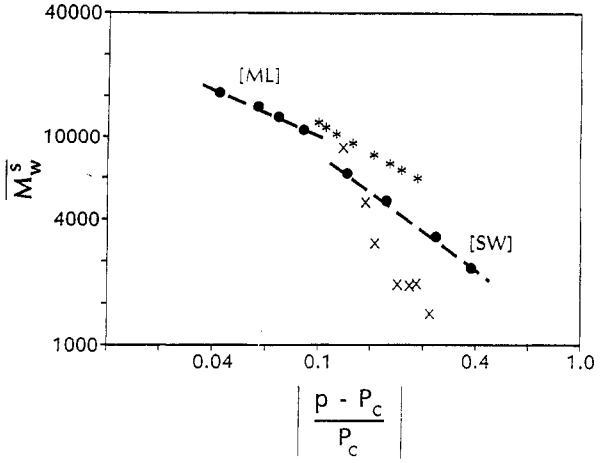

Figure 2. Evolution of the logarithm of the weight-average molecular weight, $\bar{M}_w^s$, for the sol fraction versus the logarithm of the extent of reaction, ϵ: (×) BTA/HDG in THF;[18] (●) kraft pulping of hemlock wood chips;[35] (*) Organosolv pulping of spruce meal.[33] Experimental slopes for kraft pulping of hemlock chips are shown by dashes, with middle-lamella [ML] and secondary-wall [SW] fragments identified separately.

reported by Goring[12] for viscometric data of different lignins. Values that are less than 2 may correspond to lattice animals or random walks. This would correspond to a partially degraded network similar to a crumpled sheet of paper that is more or less "smoothed out" by good solvents, whereas the conformation of a non-free-draining network is closer to that of a linear random coil with no cross-links. In the absence of chain interactions or extensive intramolecular cross-linking, a tridimensional branched polymer or vulcanizate ($D_p^* = 4$) will assume upon swelling a lattice-animal configuration, with $D_a = 2$. The degradation of such a network should also conform to Flory–Stockmayer degelation. Several examples are reported for D_v in Table VI for lignin degradation. Experimental values for ϕ are shown for comparison. A value of $\nu^* = 0.89$ was used for networks of low polydispersity. Very good agreement with D_v is obtained, a result which suggests that three-dimensional structures are present in solvated networks.

4.4. Conclusion. We have shown that applying modern gelation theories such as percolation and CCA to degradation processes during pulping represents a powerful tool toward a fundamental understanding of lignin degradation. In particular, our analysis suggests that lignin degradation can be explained as the combination of two processes: (1) the degelation of two cross-linked networks of different polydispersities and (2) the occurrence of extensive condensation reactions within the sol phase. The interaction between these effects may explain the unusual aspects of lignin degradation curves observed for different chemical pulping processes.

Acknowledgment. We thank J. T. Wearing, A. G. Robertson, and M. D. Ouchi for their timely advice, encouragement, and review of the manuscript. We acknowledge the partial support of the Science Council of British Columbia provided to Denys F. Leclerc in the form of an Industrial Post-doctoral Fellowship. We also express our appreciation for the funding provided to James A. Olson by the Natural Sciences and Engineering Research Council of Canada, through the Industrial Undergraduate Student Research Award. Special thanks must go to H. I. Bolker for his enthusiastic support and inspiration regarding percolation theory.

Nomenclature

d	network dimensionality
D_a	fractal dimension of lattice animals
D_p	fractal dimension of polydisperse clusters in percolation theory
D_v	fractal dimension of partially-swollen clusters (from viscometry)
$f(\epsilon[M_j]^\sigma)$	cutoff function for cluster-size number distribution
M^*	characteristic molecular weight of sol clusters
M_0	molecular weight of monomers
$\bar{M}_w^s$	weight-average molecular weight of sol clusters
M_j	molecular weight of a cluster having j monomers
n_j	number of clusters having a molecular weight M_j
n^*	initial number of monomers
p	probability of bond formation
P_c	critical probability for which degelation occurs
W^s	weight fraction of sol
W^g	weight fraction of gel
Z	number of monomers in cross-linking unit
α	branching coefficient
α'	Mark–Houwink exponent (conformation-dependent)
β	order-parameter exponent
γ	molecular-weight exponent
δ	density of intramolecular (cyclic) cross-links
ϵ	extent of reaction
$[\eta]$	intrinsic viscosity [cm^3/g]
ν	correlation-length exponent
ξ	radius of gyration of sol clusters [cm]
$\rho_j(\epsilon)$	cluster-size number distribution of sol fraction
σ	cutoff exponent
τ	cluster-size exponent
ϕ	fractal dimension of partially-swollen clusters in reaction bath (calculated from scaling exponents)

References and Notes

(1) Szabo, A.; Goring, D. A. I. *Tappi* **1968**, *51* (10), 440.
(2) Flory, P. J. *J. Phys. Chem.* **1942**, *46* (1), 132.
(3) Bixler, A. L. M. *Tappi* **1938**, *21*, 181.
(4) (a) de Gennes, P.-G. *J. Phys. (Paris)* **1976**, *37* (1), L1. (b) Meakin, P. *Phys. Rev. Lett.* **1983**, *51*, 1119. (c) Kolb, M.; Botet, R.; Jullien, R. *Phys. Rev. Lett.* **1983**, *51*, 1123.
(5) Procter, A. R.; Yean, W. Q.; Goring, D. A. I. *Pulp Pap. Can.* **1967**, *68*, T445.
(6) Sjostrom, E.; Sorvai, J.; Klemola, A.; Laine, J. *Nordic Pulp Pap. Res.* **1987**, *3*, 92.
(7) Paszner, L.; Behera, N. C. *Holzforschung* **1989**, *43* (3), 159.
(8) Paszner, L.; Cho, H. J. *Tappi* **1989**, *72*, 135.
(9) Wood, J. R.; Ahlgren, P. A.; Goring, D. A. I. *Sven. Papperstidn.* **1972**, *75*, 15.
(10) Kerr, A. J.; Goring, D. A. I. *Can. J. Chem.* **1975**, *53*, 952.
(11) Whiting, P.; Goring, D. A. I. *J. Wood Chem. Technol.* **1981**, *1* (2), 111.
(12) Goring, D. A. I. In *Lignins: Occurrence, Formation, Structure and Reactions*; Sarkanen, K. V., Ludwig, C. H., Eds.; John Wiley and Sons: New York, 1971; p 695.
(13) Goring, D. A. I. In *Lignin: Properties and Materials; Proceedings of the Symposium on Macromolecular Properties of Wood Biopolymers and Their Derivatives in Solution*; ACS Symposium Series 397; American Chemical Society: Washington, D.C., 1989; pp 2–10.
(14) Yean, W. Q.; Goring, D. A. I. *Pulp Pap. Can.* **1964**, *65*, T127.
(15) Ahlgren, P. A.; Yean, W. Q.; Goring, D. A. I. *Tappi* **1971**, *54* (5), 737.
(16) Favis, B. D.; Choi, P. M. K.; Adler, P. M.; Goring, D. A. I. *Trans. Tech. Sect. (Can. Pulp Pap. Assoc.)* **1981**, *7*, TR35.
(17) Johansson, A. *J. Pulp Pap. Sci.* **1986**, *11* (3), J78.
(18) Argyropoulos, D. S.; Bolker, H. I. *Macromolecules* **1987**, *20*, 2915.
(19) Kerr, A. J.; Goring, D. A. I. *Cell. Chem. Technol.* **1975**, *9*, 563.

(20) Luner, P.; Kempf, U. *Tappi* **1970**, *53* (11), 2069.
(21) Goring, D. A. I.; Vuong, R.; Gancet, C.; Chanzy, H. *J. Appl. Polym. Sci.* **1979**, *24* (4), 931.
(22) Smith, D. C.; Glasser, W. G.; Glasser, H. R.; Ward, T. C. *Cell. Chem. Technol.* **1988**, *22*, 171.
(23) Flory, P. J. *Principles of Polymer Chemistry*; Cornell University Press: Ithaca, NY, 1953; Chapter 9.
(24) (a) Fergus, B. J.; Procter, A. R.; Scott, J. A. N.; Goring, D. A. I. *Wood Sci. Technol.* **1969**, *3* (2), 117. (b) Fergus, B. J.; Goring, D. A. I. *Holzforschung* **1970**, *24* (4), 118.
(25) Berry, R. M.; Bolker, H. I. *J. Pulp Pap. Sci.* **1986**, *12* (1), J16.
(26) Stockmayer, W. H. *J. Chem. Phys.* **1944**, *12*, 125.
(27) Bolker, H. I.; Brenner, H. S. *Science (Washington, D.C.)* **1970**, *170*, 173.
(28) Argyropoulos, D. S.; Bolker, H. I. *Macromolecules* **1986**, *19*, 3001.
(29) Argyropoulos, D. S.; Bolker, H. I. *J. Wood Chem. Technol.* **1987**, *7*, 1.
(30) Argyropoulos, D. S.; Bolker, H. I. *Makromol. Chem.* **1988**, *189*, 607.
(31) Argyropoulos, D. S.; Bolker, H. I. *J. Wood Chem. Technol.* **1987**, *7*, 499.
(32) Yan, J. F. *Macromolecules* **1981**, *14*, 1438.
(33) Pla, F.; Yan, J. F. *J. Wood Chem. Technol.* **1984**, *4* (3), 285.
(34) Yan, J. F.; Pla, F.; Kondo, R.; Dolk, M.; McCarthy, J. L. *Macromolecules* **1984**, *17*, 2137.
(35) Dolk, M.; Pla, F.; Yan, J. F.; McCarthy, J. L. *Macromolecules* **1986**, *19*, 1464.
(36) Leibler, L.; Schosseler, F. *Phys. Rev. Lett.* **1985**, *55*, 1110.
(37) (a) Daoud, M.; Bouchaud, E.; Jannick, G. *Macromolecules* **1986**, *19*, 1955. (b) Daoud, M.; Martin, J. E. 3.1.1 Fractal Properties of Polymers. In *The Fractal Approach to Heterogeneous Chemistry*; Avnir, D., Ed.; J. Wiley and Sons: New York, 1989. (c) Meakin, P. 3.1.2 Simulations of Aggregation Processes. In *The Fractal Approach to Heterogeneous Chemistry*; Avnir, D., Ed.; J. Wiley and Sons: New York, 1989. (d) Vicsek, T. Cluster–Cluster Aggregation. In *Fractal Growth Phenomena*; World Scientific: Singapore, 1989; Chapter 8.
(38) Broadbent, S. R.; Hammersley, J. M. *Proc. Cambridge Philos. Soc.* **1957**, *53*, 629.
(39) (a) Stauffer, D. *J. Chem. Soc., Faraday Trans. 2* **1976**, *72*, 1354. (b) Stauffer, D.; Coniglio, A.; Adam, M. *Adv. Polym. Sci.* **1982**, *44*, 103.
(40) Essam, J. W. *Rep. Prog. Phys.* **1980**, *43*, 833.
(41) Orbach, R. *Science (Washington, D.C.)* **1986**, *231*, 814.
(42) Ord, G.; Whittington, S. G. *J. Phys. A: Math. Gen.* **1982**, *15*, L29.
(43) Chu, B.; Wu, C.; Wu, W. D.; Phillips, J. C. *Macromolecules* **1987**, *20*, 2642.
(44) (a) Li, H. *Huaxue Tongbao* **1988**, *7*, 6. (b) Daoud, M.; Family, F.; Jannink, G. *J. Phys.* **1984**, *45*, L199.
(45) Chandler, R.; Koplik, J.; Lemen, K.; Willemsen, J. *J. Fluid Mech.* **1982**, *119*, 249.
(46) Wilkinson, D.; Willemsen, J. F. *J. Phys. A: Math. Gen.* **1983**, *16*, 3365.
(47) de Gennes, P.-G. *Scaling Concepts in Polymer Physics*; Cornell University Press: Ithaca, NY, 1979.
(48) Adam, M.; Delsanti, M.; Munch, J. P.; Durand, D. *Percolation-Type Growth Clusters near the Gelation Threshold*; *Extended Abstracts, EA-13 (Fractal Aspects of Materials: Disordered Systems Proceedings of Symposium S)*; Materials Research Society: Pittsburgh, 1987.
(49) Peniche-Covas, C. A. L.; Gordon, M.; Judd, M.; Kajiwara, K. *Discuss. Faraday Soc.* **1974**, *57*, 165.
(50) Good, I. J. *Proc. R. Soc. London, Ser. A* **1963**, *272*, 54.
(51) Macosko, C. W.; Miller, D. R. *Macromolecules* **1976**, *9*, 199, 206.
(52) Gould, H.; Tobochnik, J. *An Introduction to Computer Simulation Methods: Application to Physical Systems*; Addison-Wesley: Reading, MA, 1988.
(53) Li, H. *Measurements of Fractal Dimension of Polymer Chains in Solution by Viscometry*; *Extended Abstracts EA-17 (Fractal Aspects of Materials II; Proceedings of Symposium U)*; Schaefer, D., Laibowitz, R., Mandelbrot, B., Liu, S., Eds.; Materials Research Society: Pittsburgh, 1986.
(54) Zimm, B. H.; Stockmayer, W. H. *J. Chem. Phys.* **1949**, *17*, 1301.
(55) Leibler, L.; Schosseler, F.; Benoit, H.; Collette, C.; Lafauma, F.; Robert, R. *Gelation of Polymer Solutions*; *Extended Abstracts EA-17 (Fractal Aspects of Materials II; Proceedings of Symposium U)*; Schaefer, D., Laibowitz, R., Mandelbrot, B., Liu, S., Eds.; Materials Research Society: Pittsburgh, 1986.
(56) Martin, J. E.; Keefer, K. *Intermediate Scattering Below the Sol/Gel Transition*; *Extended Abstracts EA-17 (Fractal Aspects of Materials II; Proceedings of Symposium U.)*; Schaefer, D., Laibowitz, R., Mandelbrot, B., Liu, S., Eds.; Materials Research Society: Pittsburgh, 1986.
(57) Argyropoulos, D. S.; Berry, R. M.; Bolker, H. I. *J. Polym. Sci. B: Polym. Phys.* **1987**, *25*, 1191.
(58) Gardon, J. L.; Mason, S. G. *Can. J. Chem.* **1955**, *33*, 1477.
(59) McNaughton, J. G.; Yean, W. Q.; Goring, D. A. I. *Tappi* **1967**, *50* (11), 548.
(60) Rezanowich, A.; Yean, W. Q.; Goring, D. A. I. *Sven. Papperstidn.* **1963**, *66*, 141.
(61) (a) Gupta, P. R.; Goring, D. A. I. *Can. J. Chem.* **1960**, *38*, 248. (b) Gupta, P. R.; Robertson, R. F.; Goring, D. A. I. *Can. J. Chem.* **1960**, *38*, 260.
(62) Yean, W. Q.; Rezanowich, A.; Goring, D. A. I. In *Chim., Biochim., Lignine, Cellulose et Hemicellulose*, Grenoble, 1964, p 327.
(63) Marton, J.; Marton, T. *Tappi* **1964**, *47*, 471.

Registry No. BTA/DMG (copolymer), 34606-50-3; BTA/HDG (copolymer), 104241-62-5; lignin, 9005-53-2.